

A *Drosophila* In Vivo Screen Identifies Store-Operated Calcium Entry as a Key Regulator of Adiposity

Jens Baumbach,^{1,2} Petra Hummel,³ Iris Bickmeyer,¹ Katarzyna M. Kowalczyk,^{1,5} Martina Frank,^{1,6} Konstantin Knorr,^{1,7} Anja Hildebrandt,^{1,2,8} Dietmar Riedel,⁴ Herbert Jäckle,¹ and Ronald P. Kühnlein^{1,2,*}

¹Abteilung Molekulare Entwicklungsbiologie

²Forschungsgruppe Molekulare Physiologie

³IT und Elektronik Service

⁴Facility für Elektronenmikroskopie

Max-Planck-Institut für biophysikalische Chemie, 37077 Göttingen, Germany

⁵Present address: University of Manchester, Faculty of Life Sciences, M13 9PL Manchester, UK

⁶Present address: Institut für Biochemie, Genetik und Mikrobiologie, Universität Regensburg, 93040 Regensburg, Germany

⁷Present address: Institut für Zoologie, Tierärztliche Hochschule Hannover, 30173 Hannover, Germany

⁸Present address: Abteilung Molekulare Entwicklungsbiologie, Forschungsgruppe Molekulare Organogenese, Max-Planck-Institut für biophysikalische Chemie, 37077 Göttingen, Germany

*Correspondence: rkuehnl@gwdg.de

<http://dx.doi.org/10.1016/j.cmet.2013.12.004>

SUMMARY

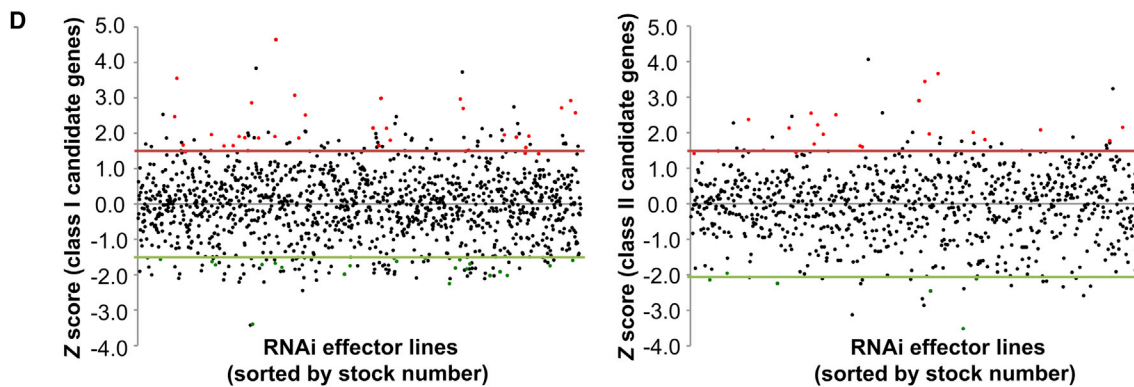
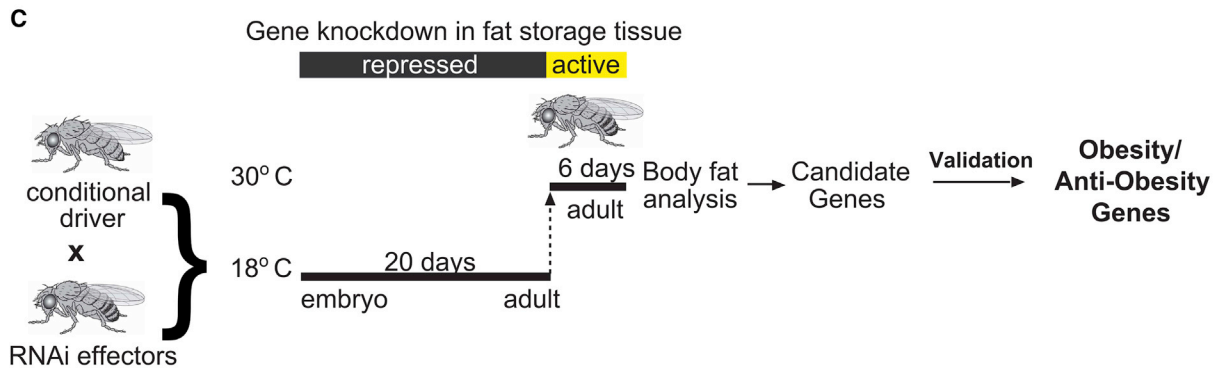
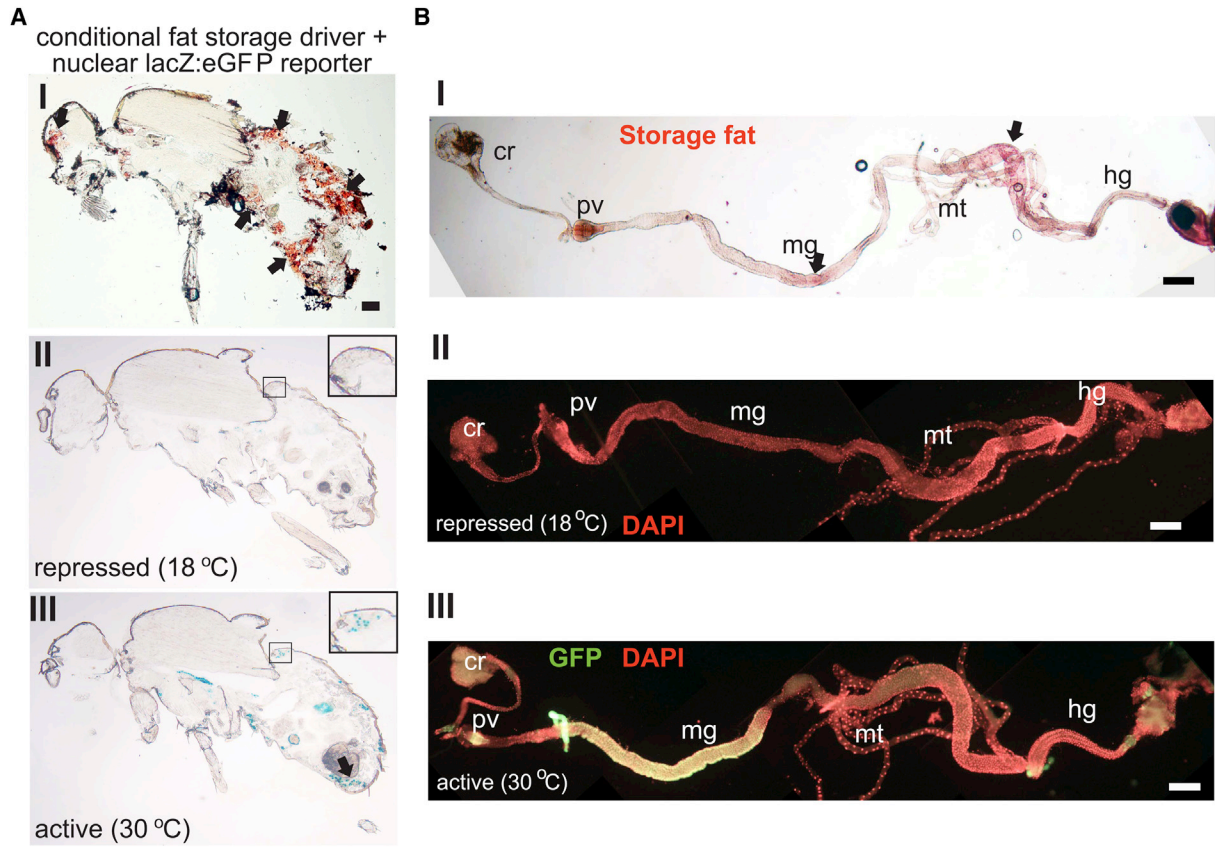
To unravel the evolutionarily conserved genetic network underlying energy homeostasis, we performed a systematic in vivo gene knockdown screen in *Drosophila*. We used a transgenic RNAi library enriched for fly orthologs of human genes to functionally impair about half of all *Drosophila* genes specifically in adult fat storage tissue. This approach identified 77 genes, which affect the body fat content of the fly, including 58 previously unknown obesity-associated genes. These genes function in diverse biological processes such as lipid metabolism, vesicle-mediated trafficking, and the universal store-operated calcium entry (SOCE). Impairment of the SOCE core component *Stromal interaction molecule (Stim)*, as well as other components of the pathway, causes adiposity in flies. Acute *Stim* dysfunction in the fat storage tissue triggers hyperphagia via remote control of the orexigenic *short neuropeptide F* in the brain, which in turn affects the coordinated lipogenic and lipolytic gene regulation, resulting in adipose tissue hypertrophy.

INTRODUCTION

Energy homeostasis is an evolutionarily conserved regulatory process that is essential for all animal organisms including human. Consistent with its ancient genetic basis, cellular lipid storage regulators are conserved from yeast to mammals (Czabany et al., 2007; Goodman, 2009; Kohlwein, 2010; Murphy, 2012; Walther and Farese, 2012; Zechner et al., 2012). Regulator mutants, which give rise to obese or lean individuals, have been identified in animal species as diverse as nematodes, insects, fish, mice, and man (Grönke et al., 2005; Haemmerle et al.,

2006; Halaas et al., 1995; Mak et al., 2006; McMenamin et al., 2013; Montague et al., 1997; Suh et al., 2007). The understanding of organismal body fat storage control is most advanced in mammals, in particular because the human obesity pandemics spurred an intensive search for obesity-associated genes (Sandholt et al., 2012). Yet, the identified obesity gene variants explain only less than 2% of the interindividual variation in body mass index (Speliotes et al., 2010). This incomprehensive identification of the genetic factors underlying adiposity can be explained by the polygenic nature of obesity (Choquet and Meyre, 2011), by the heterogeneity of genetic background within human populations, and by the complex gene-environment interactions that strongly influence disease expressivity (McAllister et al., 2009). Genetic screens in invertebrate model organisms such as yeast (Daum et al., 1999; Natter et al., 2005), *C. elegans* (Ashrafi et al., 2003), and *Drosophila* (Beller et al., 2008; Guo et al., 2008; Pospisilik et al., 2010) were successfully used to overcome some of these limitations and identified numerous genes that can affect organismal fat storage. Moreover, they revealed that many of these genes are conserved in evolution. However, none of these screens aimed yet at the identification of genes that function in an organ-specific manner in differentiated fat storage tissues of adult animals or in interorgan communication processes underlying adiposity.

We performed a large-scale *Drosophila* screen based on in vivo RNAi gene knockdowns, specifically in the fat storage tissue of the adult fly (i.e., the fat body and parts of the midgut) (Sieber and Thummel, 2009). We used a transgenic RNAi line collection enriched for orthologs of human genes and asked whether the corresponding gene knockdowns affect the accumulation of body fat in adult flies (i.e., resulted in obese or lean individuals). By screening almost half of all *Drosophila* protein-coding genes, we identified 77 total genes that function as obesity and antiobesity fly genes, of which 64 (83%) possess a human ortholog. The identified genes participate in diverse biological processes, including lipid metabolism, vesicle-mediated intracellular trafficking, and the evolutionarily conserved



(legend on next page)

store-operated calcium entry (SOCE), which acts as an adiposity regulator. Genetic interventions that reduce or increase the intracellular Ca^{2+} (iCa^{2+}) concentration in fat storage tissue rapidly cause obesity and leanness, respectively. To address the mechanisms underlying *StimKD*-dependent adiposity progression in the fly, we took advantage of the switchable knockdown system to monitor the sequence of regulatory events involved in interorgan communication. Early *Stromal interaction molecule* (*Stim*) impairment in fly fat storage tissue induces the orexigenic *short neuropeptide F* (*sNPF*) gene in the brain and causes hyperphagia, which, in turn, feeds back in adipose tissue by inducing an obesogenic gene transcription response, resulting in severe adiposity.

RESULTS AND DISCUSSION

Obesity-Associated Genes Acting in the Adult *Drosophila* Fat Storage Tissues

Drosophila offers unique options for the control of combined tissue- and time-specific gene expression control in a large-scale genetic screen format. We used the temperature-controlled in vivo TARGET system (McGuire et al., 2003) to perform gene knockdown experiments by RNAi transgene expression specifically in the two fat storage organs of the adult fly (i.e., the fat body and parts of the midgut) (Sieber and Thummel, 2009). Reporter gene expression (i.e., nuclear β -galactosidase:eGFP) shows that this conditional driver system (see Experimental Procedures) causes transgene expression exclusively in the fat storage organs at 30°C (active condition), but not at 18°C (repressed condition) (Figures 1A and 1B). To perform large-scale in vivo gene knockdowns, we combined this conditional driver system with individual transgenic RNAi effector fly lines (Dietzl et al., 2007). Flies were crossed to obtain offspring, which contained the conditional driver system combined with a single RNAi effector transgene. To prevent the functional impairment of the targeted genes prior to adulthood, the flies were raised under repressed condition. After hatching of the adults, the RNAi-dependent gene knockdown was induced in the fat storage tissues by shifting the flies to the active condition for 6 days, and the body fat content was determined (Figure 1C). Gene knockdowns that caused flies with low or high body fat content (called “lean” or “obese” flies in the following), compared to the average body fat content of all flies tested, were selected as body fat regulator candidates. These candidates were retested to confirm the results of the primary screen. We used either the average body fat content of the

primary screen candidates (class I; Figure 1D, left) or control flies, which carry the RNAi effector transgene but no driver transgene (class II; Figure 1D, right) as a reference for the body fat content. To minimize false positive identifications, we excluded candidate fly lines expressing RNAi transgenes with low target specificity, and we confirmed the candidates by experimental validation using alternative fat body driver lines and/or independent transgenic RNAi effector transgenes targeting the same gene (for details on the selection strategy, see Experimental Procedures).

We screened 7,524 RNAi effectors fly strains, which target a total of 6,796 individual genes, corresponding to 49% of all protein-coding *Drosophila* genes. After retesting and validation, we obtained 77 (1%) body fat regulator genes. Forty-seven of them cause obese flies (called “antiobesity genes” in the following), and 30 cause lean flies (called “obesity genes” in the following). The majority of the 77 identified genes (64; 83%) possess a human ortholog, and 58 genes (75%) have not been previously associated with body fat control in flies (Figures 2A and 2B; Table S1 available online).

In order to test whether the effect on body fat regulation of the genes is specific for adult fat storage tissue, we expressed the 77 RNAi transgenes in the developing fat storage tissue of larvae and pupae. Developmental impairment of almost half of the identified genes (35; 45%) caused preadult lethality (Table S1). This result suggests that the newly identified adult obesity and antiobesity genes carry developmentally relevant functions in the fly. Since the corresponding individuals never develop into adult flies, these genes would have escaped the identification as body fat regulators by conventional mutant analysis.

In order to uncover the possible biological function of the identified obesity and antiobesity genes, we employed gene ontology (GO) analysis. Fifty-five genes (71%) had at least one GO term (category “Biological function”; Table S1) and could be assigned to distinct molecular and cellular processes, such as lipid metabolism, vesicle-mediated transport, and calcium signaling (Figures 2A and 2B; Table S1). Genes involved in the lipid metabolism of the fly include previously identified key regulators of glycerolipid homeostasis, such as *Drosophila* diacylglycerol O-acyltransferase (*DmDGAT1*), encoded by the *midway* (*mdy*) gene (Buszczak et al., 2002), and the triacylglycerol (TAG) lipase, encoded by *brummer* (*bmm/DmATGL*) (Grönke et al., 2005), an ortholog of the mammalian *adipose triglyceride lipase* (Zimmermann et al., 2004) (Figures 2 and S1). The body fat storage phenotypes of the *mdy* and *bmm* conditional RNAi knockdown flies and the respective mutants are indistinguishable

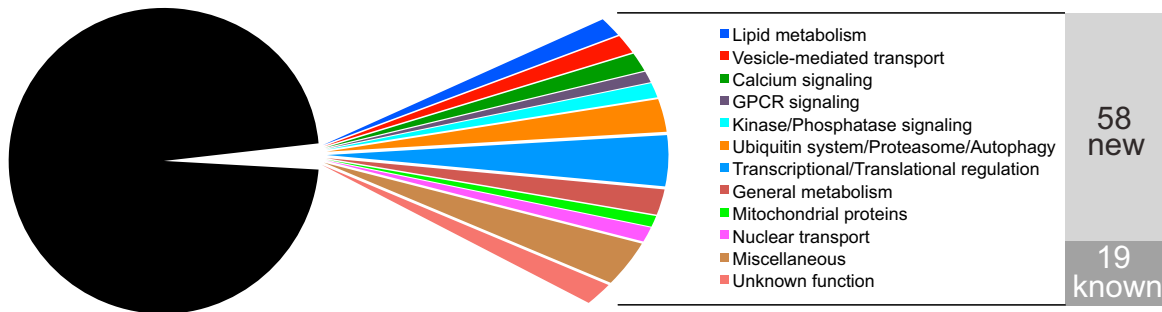
Figure 1. Experimental Approach of the Fat-Storage-Tissue-Specific In Vivo Knockdown Screen and Selection Strategy for Fly Obesity and Antiobesity Genes

(A and B) Storage fat distribution (AI) and conditional β Gal:eGFP reporter expression (AII repressed condition; AIII active condition) in the head and abdominal fat body (arrows in [A] or intestine [B]) of adult male flies; scale bar equals 200 μm ; cr indicates crop, pv indicates proventriculus, mg indicates midgut, mt indicates Malpighian tubules, and hg indicates hindgut; note nuclear counterstaining [DAPI] in AII and AIII).

(C) Workflow of the fly obesity and antiobesity gene identification scheme. Candidate genes were identified after two rounds of screening (primary and secondary) based on changes of the body fat content in response to adult fat-storage-tissue-targeted gene knockdown. Obesity and antiobesity genes were selected among the candidate genes by a restrictive in silico and experimental validation scheme (for details see Results and Experimental Procedures).

(D) Graphical representation of the final candidate gene identification based on body fat changes relative to all primary screen candidates (class I; left) or to individual controls (class II; right). Shown are plots of Z scores for all primary candidate fly lines subjected to class I or class II selection criteria with the thresholds for obese (red lines) and lean (green lines) candidate genes, respectively. Fly lines, which represent validated antiobesity (red) and obesity (green) genes, are highlighted by dots. See also Table S1.

A 6796 genes screened → 47 Anti-Obesity and 30 Obesity genes (total 77)



B

Functional class **Anti-Obesity gene/short name** or **Obesity gene/short name (human ortholog)**

■ Lipid metabolism

Adipokinetic hormone receptor/AkhR (GNHRH), midway/mdy (DGAT1), CG14512
brummer/bmm (ATGL), Phosphoethanolamine cytidyltransferase/Pect (PCYT2)

■ Vesicle-mediated transport

ADP ribosylation factor 79F/Art79F (ARF1), sec71 (ARFGEF1/2), stenosis/sten (SEC24C), CG5484 (YIF1B), Ykt6

■ Calcium signaling

Calmodulin/Cam (CALM), purity of essence/poe (UBR4), Calcium ATPase at 60A/Ca-P60A (ATP2A2), olf186-F (ORAI3)
Stromal interaction molecule/Stim (STIM1)

■ GPCR signaling

G protein α49B/Gα49B (GNAQ), G protein γ 1/Gy1 (GNG12), Leucine-rich repeat-containing G protein-coupled receptor 1/Lgr1 (LHCGR)

■ Kinase/Phosphatase signaling

CG9238 (PPP1R3C), multiple ankyrin repeats single KH domain/mask (ANKHD1), punt/put (ACVR2), CG16903 (CCNL1)

■ Ubiquitin system/Proteasome/Autophagy

COP9 complex homolog subunit 4/CSN4 (COPS4), Aut1 (ATG3), Ecdysone-induced protein 74EF/Eip74EF, Proteasome α5 subunit/Prosa5 (PSMA5), Proteasome β3 subunit/Prosβ3 (PSMB3), Regulatory particle non-ATPase 6/Rpn6 (PSMD11), Regulatory particle non-ATPase 7/Rpn7 (PSMD6), Regulatory particle non-ATPase 8/Rpn8 (PSMD7), Fbw5 (FBXW5)

■ Transcriptional/Translational regulation

bip2 (TAF3), Retinal Homeobox/Rx, Rpd3 (HDAC2), split ends/spen (SPEN), Br140 (BRD1), CG6272 (CEBPG), CG6937 (MKI67IP), Es2 (DGCR14), held out wings/how (QKI), ftz transcription factor 1/ftz-f1 (NR5A2), Eukaryotic initiation factor 1A/eIF-1A (EIF1AX), Suppressor of variegation 3-9/Su(var)3-9 (SUV39H2), Ribosomal protein L26/RpL26 (RPL26L1), lethal (2) NC136/l(2)NC136 (CNOT3)

■ General metabolism

antdh (DHRS11), Carbonic anhydrase 2/CAH2, Tyramine β hydroxylase/Tbh (DBH), CG10166 (DPM1), CG15890, CG31915 (COLGALT2), CG9940 (NADSYN1)

■ Mitochondrial proteins

tamas/tam (POLG), CG4743 (SLC25A26), CG3214 (NDUFA12)

■ Nuclear transport

Cullin-4/Cul-4 (CUL4B), CAS/CSE1 segregation protein/Cas (CSE1L), Megarot/Mtor (TPR), Nuclear transport factor-2/Ntf-2 (NUTF2)

■ Miscellaneous

Na,K-ATPase Interacting/NKAIN, Related to the N terminus of tre oncogene/RN-tre (TBC1D3), Vacuolar H⁺ ATPase M8.9 accessory subunit/VhaM8.9 (ATP6AP2), Vacuolar H⁺ ATPase subunit 16-1/Vha16-1 (ATP6V0C), CG7379 (ING2), CG7770 (PFDN6), unc-45 (UNC45B), CG6750 (EMC3), CG14210, Lasp, pecanex/pcx (PCNXL), pollux/plx

■ Unknown function

CG15142, lethal (2) 05714/l(2)05714, lethal (3) 05822/l(3)05822, CG14270 (C19orf52), CG3500 (TEX261), CG15618 (THADA)

(legend on next page)

(Figures S1A–S1C). These observations confirm the tissue-specific role of the genes in adult flies and emphasize the validity of the screening approach.

In addition to glycerolipid metabolism genes, we also identified a key regulator of the phospholipid biosynthesis, *Pect* (also referred to as *DmPCYT2*), as antiobesity gene (Figures 2B and S1D–S1G). *Pect* encodes phosphoethanolamine (PE) cytidyltransferase, the fly homolog of mammalian *PCYT2*. It catalyzes the rate-limiting step in the CDP-ethanolamine pathway of PE synthesis (Fullerton et al., 2009), which requires diacylglycerol (DAG), an intermediate of the Kennedy pathway required for TAG biosynthesis. Thus, *Pect* links the phospholipid and the glycerolipid metabolism (Figure S1D). Consistent with this functional assignment, *Pect* knockdown in adult fat storage tissue increases the TAG and DAG contents (Figures S1E–S1G) and enhances *mdy/DmDGAT1* gene expression (Figure S1H). Moreover, *Pect* knockdown flies display the transcriptional signature of increased lipogenesis by upregulating the *Fatty acid synthase (Fas)*, *Acetyl-CoA carboxylase (ACC)*, and *Acetyl Coenzyme A synthase (ACS)* genes (Figure S1H). This finding supports earlier studies, showing that an impairment of PE biosynthesis (i.e., by mutations in the ethanolamine kinase gene *easily shocked* or due to global *Pect* knockdown) causes lipotoxic cardiomyopathy and obesity in flies (Lim et al., 2011). The coupling of the phospholipid and glycerolipid metabolisms appears to be conserved between flies and mammals, since heterozygous *PCYT2* knockout mice develop obesity (Fullerton et al., 2009), and hepatocyte-specific *PCYT2* knockout mice suffer from liver steatosis (Leonardi et al., 2009). In both cases, lipogenic genes are upregulated (Fullerton et al., 2009; Leonardi et al., 2009), as observed in flies.

GO analysis indicates that genes involved in vesicle-mediated transport between endoplasmic reticulum (ER) and Golgi participate in adiposity control (Figure 2). Among those genes, *ADP ribosylation factor at 79F (Arf79F)* and *sec71* act as antiobesity genes (Figures S1I–S1K). ARF79F is the fly ortholog of mammalian ARF1, a small GTPase required for Golgi integrity. ARF1 acts as key regulator of COPI-mediated retrograde transport between Golgi and ER and is regulated by the guanine nucleotide exchange factors (GEFs) ARFGEF1 and ARFGEF2 at the *trans*-Golgi. Impairment of the *Drosophila* ARFGEF1/2 homolog encoded by *sec71* in the fat body causes adiposity in flies (Figures S1I–S1K), as do knockdowns of the COPII-dependent vesicle trafficking component SEC24 encoded by the *stenosis* (or *ghost*) gene and the R/v-SNARE *Ykt6*, which functions in ER-Golgi trafficking (McNew et al., 1997). *Ykt6* orthologs participate in macroautophagy (Nair et al., 2011). In fact, macroautophagy of lipid droplets has been described as a key process in regulating the cellular fat storage homeostasis in mammals (Singh et al., 2009). Furthermore, vesicle-mediated trafficking regulators are known to participate in cellular lipid accumulation

(Beller et al., 2008; Guo et al., 2008). The identification of already known and additional vesicle-mediated trafficking regulators in our screen emphasizes the importance of cellular trafficking processes in adipocytes for the organismal fat storage homeostasis.

Body Fat Control by SOCE

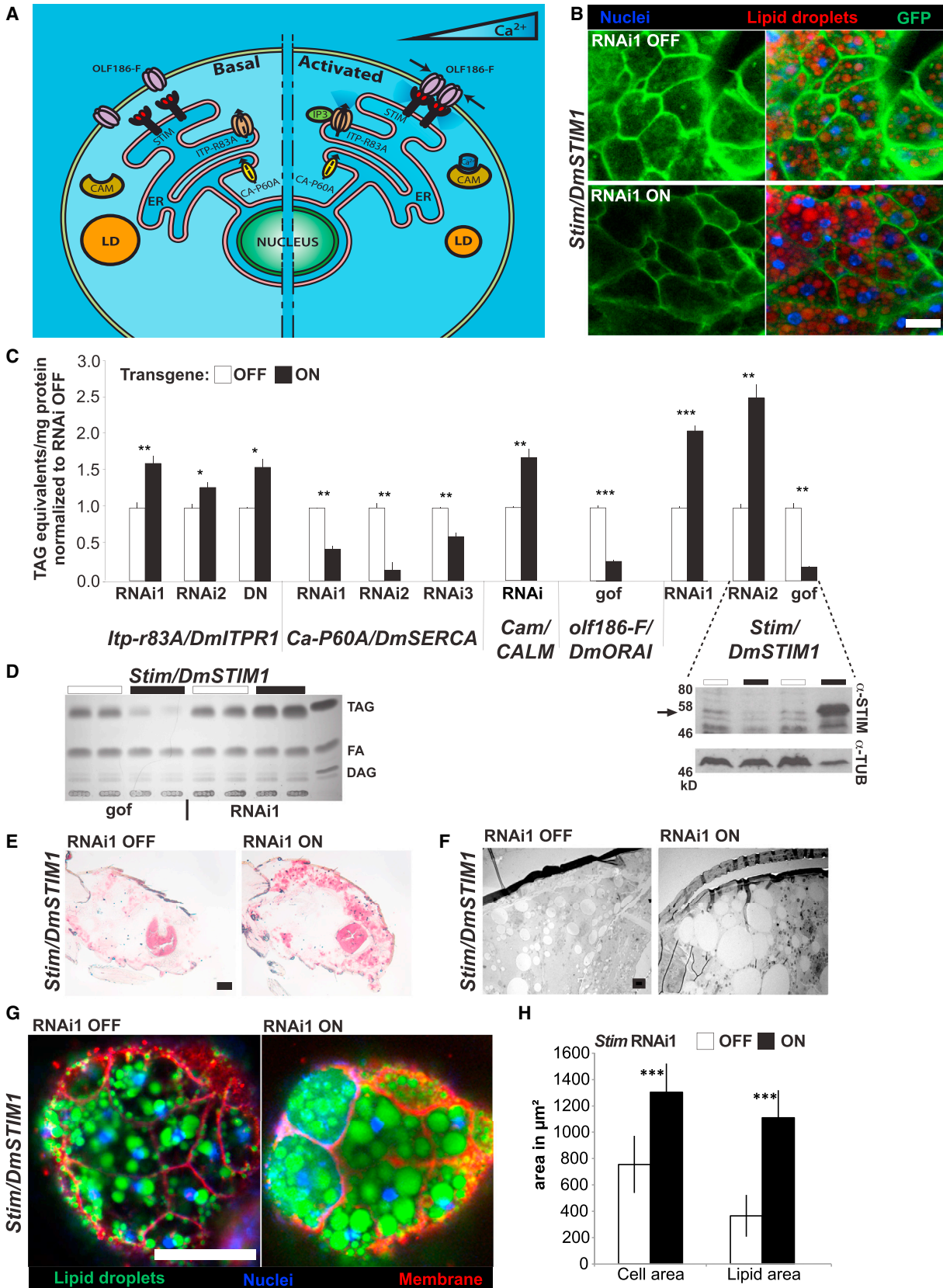
Regulation of ion transport is the most prominent GO term among the newly identified adiposity genes (Table S1), including genes that encode core components of the SOCE (Figure 2). Canonical SOCE (Figure 3A) is initiated by the activation of the inositol 1,4,5-tris phosphate (IP3) receptor (ITP-R83A/*DmITPR1*) at the ER. This activation causes a primary Ca^{2+} efflux from the ER to the cytoplasm, which in turn activates the ER calcium sensor encoded by the *Stim* gene. Activated STIM then interacts with the plasma membrane Ca^{2+} channel OLF186-F/*DmORAI* to further elevate the cytoplasmic calcium concentrations from extracellular pools. High intracellular Ca^{2+} (iCa^{2+}) concentrations trigger a plethora of downstream effectors, such as Calmodulin (CAM). The Ca^{2+} efflux from the ER is counteracted by the calcium pump *Ca-P60A/DmSERCA* and accordingly helps to terminate the SOCE activity (Soboloff et al., 2012).

To in vivo visualize cytoplasmic iCa^{2+} concentrations of adult fat body cells, we used the CaLexA system. It translates the iCa^{2+} concentrations to transcriptional activity of a GFP reporter gene via the Ca^{2+} -dependent nuclear import of a synthetic transcription factor (Masuyama et al., 2012). Figure 3B shows a reduction of plasma-membrane-targeted GFP in fat body cells after the *Stim* gene knockdown, indicating a depletion of iCa^{2+} in response to the SOCE impairment. Genetic manipulations of SOCE genes, which decrease the iCa^{2+} concentration in fat storage cells, such as knockdown of *Stim* or *Itp-r83A* and the overexpression of a dominant-negative form of *Itp-r83A*, cause a massive increase of the body fat content (50%–150%) and a corresponding accumulation of subcuticular body fat in flies (Figures 3C–3E and S2). Conversely, an increased iCa^{2+} concentration in fat storage cells caused by the knockdown of *Ca-P60A* or the targeted overexpression of *olf186-F* and *Stim*, respectively, results in the reduction of the body fat content of the flies by up to 85% and depletes the subcuticular abdominal lipid stores (Figures 3C, 3D, S2A, and S2B). A recent study showing that the obese phenotype of *Itp-r83A* mutants can be partially rescued by *Itp-r83A* expression in the fat body (Subramanian et al., 2013) supports the participation of SOCE genes in adiposity regulation. Knockdown of the SOCE-downstream mediator *Cam* gene increases the total body fat stores by more than 50% (Figure 3C). These findings support the conclusion that the SOCE machinery, of which the key components were identified in our screen, carries an important role in the control of adiposity.

Figure 2. Numeric Representation and Functional Classification of the *Drosophila* Antiobesity and Obesity Genes Identified by the Large-Scale, Conditional Gene Knockdown Screen

(A) Identification of 47 antiobesity genes and 30 obesity genes (total 77; 1%) among 6,796 genes analyzed in the screen; 58 (75%) of those genes are new regulators of the body fat content. Functional classification (in colors) of all obesity and antiobesity genes based on manually edited gene ontology term assignments.

(B) Full and short names of all identified *Drosophila* antiobesity genes (red) or obesity genes (green) and their respective human orthologs (black in parenthesis) organized in functional classes corresponding to (A). See also Figure S1.



Adiposity by SOCE Dysfunction in Fat Storage Tissue Involves Orexigenic Brain *sNPF* Signaling

In order to examine the role of SOCE in adiposity, we focused on the characterization of *Stim* gene function. After 6 days of *Stim* gene knockdown in the fat storage tissue (*Stim* RNAi ON; the corresponding flies are called “*Stim*KD” in the following), the STIM protein and the iCa^{2+} concentration in the fat storage cells are significantly reduced (Figures 3B, 3C, and S3A). The body fat of these flies is more than doubled, and subcuticular fat stores are increased as compared to the control flies (*Stim* RNAi OFF) (Figures 3C–3E). At the cellular level, the lipid droplet size, the total lipid droplet area, and the overall size of fat body cells are significantly increased (Figures 3F–3H). *Stim*KD-dependent obesity can be triggered in both mature adult male and female flies of different ages by different *Stim* RNAi transgenes and also in response to different transgene systems, including a temperature-independent switchable driver in adipose tissue (Figures 3C and S3B). In contrast, carbohydrate homeostasis is not affected by the *Stim* impairment, since the hemolymph concentrations of the circulating sugars trehalose and glucose (Figure 4A), the body content of the storage carbohydrate glycogen, and the starvation-induced glycogen mobilization profile of the *Stim*KD-dependent obese flies did not differ from control flies (Figure 4B). Normal dietary sugar responsiveness of the *Stim*KD-dependent adiposity adds further support to the conclusion that the carbohydrate metabolism is fully functional in *Stim*KD flies (i.e., these flies accumulate more body fat in response to increasing dietary sugar concentrations compared to controls) (Figure 4C). Thus, the *Stim*KD in the fat storage tissue impairs only the lipid metabolism component of energy homeostasis control. In contrast to mature adult flies (6 days after hatching), however, the *Stim* knockdown in the fat storage tissues of third instar larvae or immature adult flies (4 hr after hatching) has no significant effect on the body fat content (Figure S3C). This observation indicates that *Stim* has a specific function in regulating the energy intake and/or expenditure of the adult fly, likely related to the adult lifestyle.

To address this point, we profiled the physiological basis of obesity progression in mature adult *Stim*KD flies. While *Stim*KD flies develop severe adiposity, their locomotor activity was unchanged when compared to the control flies (Figure 4D). Moreover, measurements of CO₂ production indicate that the metabolic rate of obese *Stim*KD flies did not differ from control flies (Figure S3D). Thus, reduced energy expenditure can be excluded as a major cause of *Stim*KD-dependent obesity. We

observed, however, that the body fat content increases rapidly after *Stim*KD induction (Figure 4D), and flies become hyperphagic as early as 2 days after *Stim*KD induction (Figure 4E). Under ad libitum feeding conditions, the food intake increases steadily up to more than twice over control values from day four onward. However, when *Stim*KD flies were pair-fed (i.e., that they were restricted to the food intake of normophagic control flies), *Stim*KD flies accumulate only slightly more body fat than control flies (Figure 4F). These results support the argument that the adiposity of *Stim*KD flies is driven by hyperphagia.

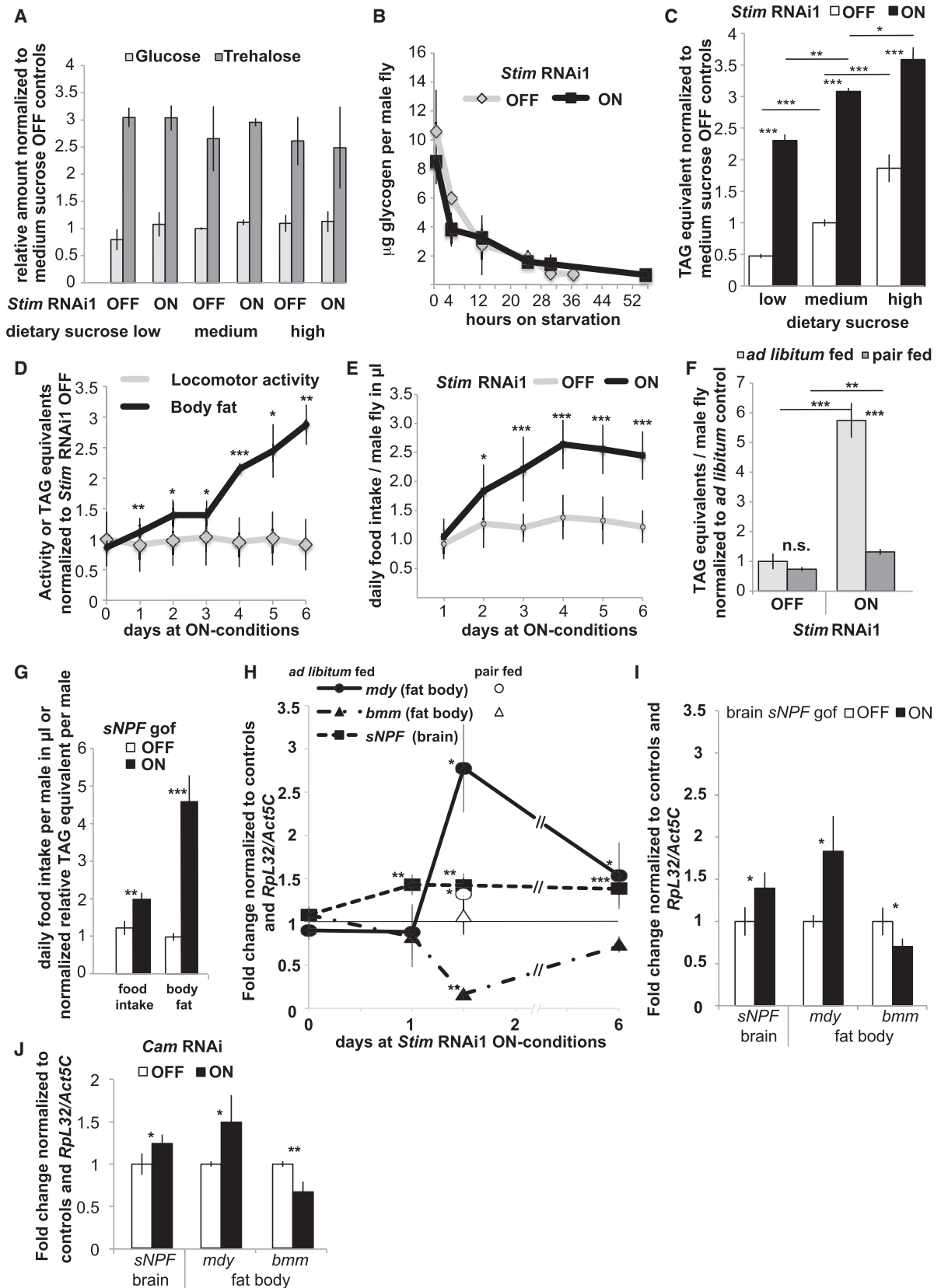
Hyperphagia indicates the lack of proper food intake control by the central nervous system. We therefore set out to reveal the regulatory events underlying adiposity progression in flies, where *Stim* activity was impaired in the fat storage tissue. We first addressed the transcriptional profile of the lipid metabolism effectors *mdy/DmDGAT1* and *bmm/DmATGL* in fat storage tissue and the orexigenic *sNPF* gene in the brain. *sNPF* is a functional homolog of mammalian orexigenic neuropeptide Y (Nässel and Wegener, 2011), and its overexpression in *sNPF*-producing neurons causes hyperphagia and body fat accumulation in flies (Figure 4G). This observation suggests *sNPF* as a plausible candidate factor to relay *Stim*KD-dependent food intake control. As shown in Figure 4H, the expression levels of *sNPF*, *mdy*, and *bmm* are not different compared to controls prior to *Stim*KD induction. However, as early as 1 day after functional impairment of *Stim* in the fat storage tissue, *sNPF* is upregulated by 42% in the brain, while fat body *mdy* and *bmm* expression are still unchanged. Even 10 hr later, *sNPF* continues to be upregulated in the brain, but the fat storage tissue now shows an obesogenic transcriptional response (i.e., the transcript abundance of *mdy* is increased by 178%, whereas *bmm* is decreased by 84%). During further progression of adiposity until day six, when the body fat content of *Stim*KD flies has more than doubled as compared to control flies (Figure 4D), *sNPF* is still upregulated in the brain. However, the *Stim*KD-dependent effects on *mdy* and *bmm* expression are less pronounced than 1 day after *Stim* impairment. The temporal sequence of transcriptional regulation suggests that *Stim* dysfunction in the fat storage tissue controls *sNPF* activity in the brain, which in turn causes hyperphagia, resulting in the obesogenic transcriptional response back in the fat body. In fact, *sNPF* overexpression in the brain of control flies has the same effect on *mdy* and *bmm* expression as observed with *Stim*KD flies (Figure 4I). Conversely, the obesogenic transcriptional response in the fat body is blunted in pair-fed *Stim*KD flies, which accumulate only slightly more body fat

Figure 3. Body Fat Control by SOCE

(A) Model of the canonical SOCE signaling in basal (left) and activated (right) states. SOCE activation increases the iCa^{2+} concentration, which activates effectors such as Calmodulin (CAM) and reduces cellular fat stores (LD indicates lipid droplet).

(B–G) Low iCa^{2+} concentration in adult fly adipose tissue upon knockdown of the SOCE ER Ca^{2+} sensor *Stim* (ex vivo imaging using the CaLexA system, based on the Ca^{2+} -dependent transcription of membrane-targeted GFP reporter protein). Left panel GFP channel; right panel overlay with lipid droplets (red) and nuclei (blue) staining. Modulation of adult male fly body fat content in response to adipose tissue manipulation of SOCE core genes *Itp-r83A/DmITPR1*, *Ca-P60A/DmSERCA*, *olf186-F/DmORAI*, and *Stim* and of *Cam* gene expression, assayed by total body fat analysis (C), thin-layer chromatography (D), and oil red O staining on sagittal cryosections of adult male fly abdomen (E) (note that homogenous oil red O staining in the ejaculatory bulb is unrelated to fat body). Changes in STIM protein abundance in fly abdomen after adipose-tissue-targeted *Stim* RNAi and *Stim* overexpression documented by western blot analysis (C). Increase in lipid droplet size and total lipid and cell area in adult male fat body cells subjected to in vivo *Stim* gene knockdown assayed by electron microscopy (F) and confocal fluorescence microscopy (G) (lipid droplets are green, nuclei are blue, and membranes are red).

(H) Lipid and total cellular area quantification of cells represented in (G). For abbreviations, DN indicates dominant negative and gof indicates gain-of-function. Error bars represent SD. * $p \leq 0.05$, ** $p \leq 0.01$, and *** $p \leq 0.001$; scale bar represents 20 μm in (B), 100 μm in (E), 4 μm in (F), and 50 μm in (G). Note that *Itp-r83A* was not included in the primary screen collection but was independently identified as an antiobesity gene using the same validation criteria. See also Figure S2.



(legend on next page)

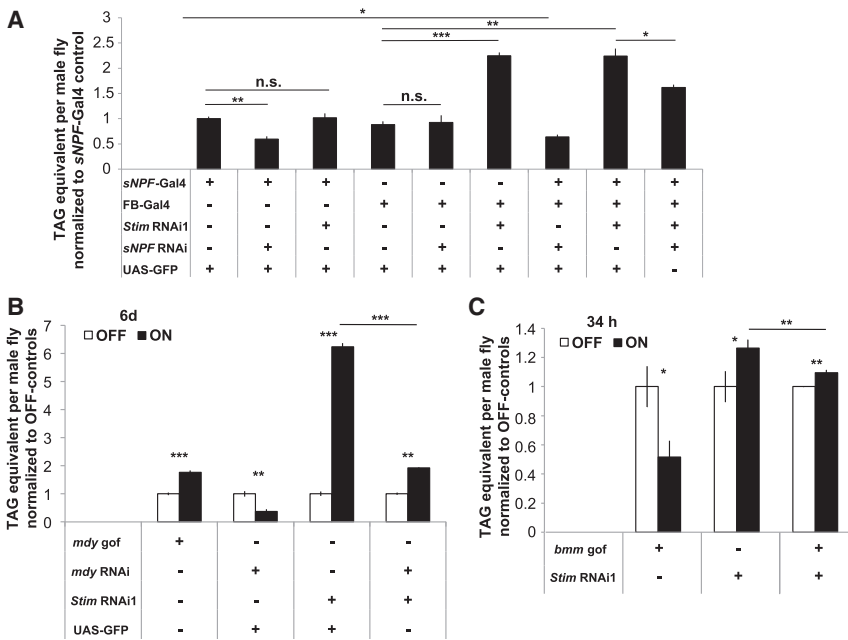


Figure 5. Transgenic Correction of *sNPF*, *mdy*, and *bmm* Gene Dysregulation Suppresses *StimKD*-Dependent Adiposity

Shown are changes in total body fat content of male flies.

(A) Attenuated adiposity in *StimKD* flies in response to simultaneous *sNPF* knockdown in the *sNPF*-positive neurons. Individual gene knockdown of *sNPF* in the brain causes leanness. No effect on body fat upon *Stim* knockdown in *sNPF*-positive neurons or *sNPF* knockdown in the fat storage tissue. FB-Gal4 indicates fat-body-Gal4.

(B) Strong suppression of *StimKD*-dependent adiposity by simultaneous *mdy* gene knockdown in the fat storage tissue. Adiposity and leanness of flies subject to fat-storage-tissue-targeted individual *mdy* gene overexpression and knockdown, respectively.

(C) Attenuated onset of *StimKD*-dependent adiposity by simultaneous *bmm* gene overexpression (*gof*) in the fat storage tissue. *bmm* gene overexpression causes leanness in control flies. Note that fly body fat content was determined after constitutive (A), conditional 6-day (B) or conditional 34-hr (C) knockdown of the respective genes. Note that a control (UAS-GFP) was used to match the number of effector transgenes. Error bars represent SD. * $p \leq 0.05$, ** $p \leq 0.01$, *** $p \leq 0.001$. n.s. indicates "not significant." See also Figure S4.

compared to controls (i.e., the *bmm* gene expression is unaffected, and *mdy* is only weakly upregulated) (Figure 4H). Collectively, these data suggest that *StimKD* in the fat body upregulates *sNPF* in the brain, which triggers hyperphagia, leading to *mdy* and *bmm* gene regulation back in the fat storage tissue. Since the fat-storage-tissue-targeted knockdown of *Cam* alters the *sNPF*, *mdy*, and *bmm* expression as observed with *StimKD* flies (Figure 4J), it is likely that *Cam* participates in the interorgan feedback control via *sNPF* signaling.

To further address the functional implication of the *sNPF*, *mdy*, and *bmm* gene regulation in *StimKD*-dependent adiposity, we first analyzed the body fat content of flies when these three genes were altered according to the effects observed in *StimKD* flies. Overexpression of *sNPF* in the brain, overexpression of *mdy* in the fat body, and *bmm* gene knockdown in the fat body cause adiposity, as observed with *StimKD* flies (Figures 5A–5C and S1A). In order to test whether *StimKD*-dependent transcrip-

tional dysregulation is indeed mediated by *sNPF* in the brain, we simultaneously impaired *sNPF* and *Stim* in brain and fat body. In such flies, *StimKD*-dependent adiposity is reduced (Figure 5A). Furthermore, simultaneous knockdown of both *mdy* and *Stim* in the adipose tissue, which counteracts the *StimKD*-induced upregulation of *mdy*, largely represses *StimKD*-dependent adiposity (Figure 5B). Moreover, overexpression of *bmm* in the adipose tissue of *StimKD* flies, which counteracts the *StimKD*-induced downregulation of *bmm*, reduces *StimKD*-dependent adiposity (Figure 5C).

These results indicate that the *StimKD*-dependent regulation of *mdy* and *bmm* expression in fat storage tissue requires *sNPF* activity in the brain and that *Stim* does, at least in part, act in a non-tissue-autonomous manner in body fat storage control (Figure 5A). The data are consistent with a model suggesting that an impairment of *Stim* in the fat storage tissue initiates *sNPF* upregulation in the central nervous system and

Figure 4. Physiology, Hyperphagia, and Fat Body—Brain Organ Communication in *StimKD*-Dependent Obesity

(A–C) Normal carbohydrate metabolism in obese *StimKD* flies. Euglycemia (A), normal glycogen storage and glycogen mobilization (B), and normal body fat response to dietary sugar (C) in obese *StimKD* flies, compared to controls. Shown are circulating hemolymph sugar (glucose and trehalose) levels (A) and total body fat content (C) of adult male flies on diets of varying sugar concentrations. Total body glycogen content and mobilization in (B) was determined for adult male flies at the onset and during a water-only starvation paradigm. (Note that the last glycogen value represents live flies scored at LD50.)

(D–F) Correlation of adiposity progression and hyperphagia in *StimKD* flies.

(D) Total body fat increase starting as early as day one after *StimKD* induction in the fat storage tissue. (Note no change in spontaneous locomotor activity during adiposity progression.)

(E) Early onset hyperphagia after *StimKD* induction in the fat storage tissue.

(F) Pair-feeding of *StimKD* flies with normophagic control flies largely suppresses *StimKD*-dependent obesity.

(G) Hyperphagia and adiposity in response to overexpression of *sNPF* in the *sNPF*-positive neurons of the brain.

(H) Upregulation of brain *sNPF* precedes the upregulation or downregulation of lipogenic *mdy* and lipolytic *bmm* gene expression, respectively, in response to *StimKD* in the fat storage tissue. Pair-feeding largely suppresses the *StimKD*-dependent obesogenic regulation of *mdy* and *bmm*.

(I) Overexpression (*gof*) of brain *sNPF* causes obesogenic *mdy* and *bmm* gene regulation, as does fat-storage-tissue-targeted *StimKD*.

(J) *Cam* is involved in interorgan communication of body fat control. Upregulation of *mdy* and brain *sNPF* expression and downregulation of *bmm* gene expression in obese flies caused by fat-storage-tissue-targeted *Cam* knockdown. Error bars represent SD. * $p \leq 0.05$, ** $p \leq 0.01$, and *** $p \leq 0.001$. See also Figure S3.

thereby causes hyperphagia. In turn, hyperphagia then triggers an obesogenic program in the fat storage tissue.

Interestingly, mammalian *Stim1* has been shown to suppress the differentiation of 3T3-L1 preadipocytes (Graham et al., 2009). Conversely, pharmacological elevation of the iCa^{2+} concentrations, either in response to the activated transient receptor potential vanilloid-1 calcium channel or by the SERCA inhibitor thapsigargin, inhibits the differentiation of 3T3-L1 and human preadipocytes into functional adipocytes (Ntambi and Takova, 1996; Zhang et al., 2007; Shi et al., 2000). However, elevation of iCa^{2+} has several effects described for mammalian adipocytes. It promotes human adipocyte maturation during late differentiation phases (Shi et al., 2000), inhibits lipolysis in human adipocytes (Xue et al., 1998), and increases lipid storage by upregulation of lipogenic genes in mature 3T3-L1 adipocytes (Jones et al., 1996). Given those cell-autonomous roles of iCa^{2+} in the mammalian fat storage cells, the possible evolutionarily conserved role of SOCE members in flies and mammals in the regulation of fat storage control has to await future studies addressing the function in mammalian organism rather than in tissue culture. It will also be of interest to elucidate the mechanisms by which interorgan communication in *StimKD*-dependent adiposity is mediated and to identify the components involved in the signaling from adipose tissue to the brain and vice versa.

In *Drosophila*, fat body signaling to the brain integrates information on nutrition, metabolism, and systemic growth (Britton and Edgar, 1998; Colombani et al., 2003; Géminard et al., 2009). In this interactive pathway, the fat-body-expressed cytokine Unpaired 2 (*Upd2*) acts as a functional homolog of mammalian leptin, which signals the “fed state” to the central nervous system via remote control of *Drosophila* insulin-like peptide (DILP) release in the brain (Rajan and Perrimon, 2012). Flies subjected to an *upd2* knockdown in the fat body are normophagic, hyperglycemic, and lean and accumulate DILP2 protein in the brain insulin-producing cells (IPCs), suggesting reduced systemic insulin signaling in such flies (Rajan and Perrimon, 2012). In the abdomen of obese *StimKD* flies, where most fat body tissue resides, *upd2* is downregulated close to half (Figure S4A). In contrast to *upd2* knockdown flies, *StimKD* flies are hyperphagic, euglycemic, and have significantly lower DILP2 accumulation in IPCs compared to controls (Figures S4B and S4C). Hence, *upd2* is not the mediator of interorgan information between fat body and brain of *StimKD* flies. The factor(s) and mechanisms underlying this process in *StimKD*-dependent adiposity are currently unknown.

Similar to its mammalian homolog NPY, *sNPF* is a critical regulator of food intake, acting in the central nervous system of the fly. Upregulation of *sNPF* gene expression in the brain of *StimKD* flies (Figure 4H) or by starvation of wild-type flies (Hong et al., 2012) increases the food intake leading to body fat accumulation under ad libitum feeding conditions (Figure 4G). Conversely, downregulation of the gene in *sNPF*-positive neurons reduces food intake (Lee et al., 2004), increases starvation sensitivity (Kahsai et al., 2010), and causes lean flies (Figure 5A). Interestingly, the delicate control of the *sNPF* gene expression level is subject to an evolutionarily conserved autoregulatory loop in the brain (Hong et al., 2012). Murine *NPY* or fly *sNPF* signaling upregulates the dual specificity tyrosine-phosphorylation-regu-

lated kinase 1 (*Dyrk1*). *Dyrk1* activates the transcription factor FOXO by sirtuin-dependent deacetylation, which in turn increases *NPY* and *sNPF* expression in the brain. Thus, it is conceivable that aspects of *StimKD*-dependent adiposity regulation that include interorgan communication are conserved up to mammals.

Our screen was designed to identify body fat regulators required in the fat storage tissue of adult flies. We isolated a number of already known fly antiobesity and obesity genes, providing the proof of concept for the validity of the screening approach taken. Importantly, we found 58 previously unknown body fat regulator genes, including 46 (79%) which are sequence conserved in evolution up to humans. In addition to enzymes acting in lipid metabolism and components of the intracellular vesicle trafficking, our screen also identified the key components of the SOCE machinery, which controls the iCa^{2+} homeostasis. Calcium signaling was previously shown to participate in cell-autonomous processes of mammalian lipid metabolism. Our results provide evidence that in the fly organism, changes in the SOCE-dependent iCa^{2+} levels in fat storage cells act in a non-tissue-autonomous manner by using an as-yet-unknown interorgan communication pathway to enhance *sNPF* expression in the brain. Since the energy expenditure of such flies does not change, it is conceivable that the excess food intake causes the observed changes in gene activities, leading to a rapid increase of fat storage. Our identification of previously unknown obesity and antiobesity genes of the fly, and the non-cell-autonomous function of the SOCE machinery, now pave the way to address key questions regarding the orchestration of energy homeostasis in flies, to elucidate the fat-tissue-brain communication process, and to address questions concerning the evolutionary conservation of the factors and mechanisms underlying fat storage control in animal organisms.

EXPERIMENTAL PROCEDURES

Fly Stocks and Husbandry

Transgenic RNAi fly strains used in this study were received from either the VDRC (GD and KK library; Dietzl et al., 2007; <http://stockcenter.vdrc.at/>) or the BDSC (Harvard TRiP library; www.flyrnai.org). Unless stated differently, the flies were propagated as described (Grönke et al., 2005). If not noted otherwise, transgene ON versus OFF conditions refer to flies carrying the effector transgene in the presence and absence of a driver transgene, respectively. For details on all fly stocks and fly husbandry see Supplemental Experimental Procedures.

Histology, Microscopy, and Image Analysis

Bright-field and epifluorescence microscopies of adult fly guts were done on a Zeiss Axiophot equipped with a ProgRes 3012 camera or a Zeiss Axiovert 200M with a Hamamatsu ORCA ER camera. A Zeiss LSM 780 was used for confocal fluorescence microscopy on adult fat body tissue, for DILP2 (Géminard et al., 2009) immunocytochemistry, and for scoring of the *CaLexA* (Masuyama et al., 2012) reporter system. Images were analyzed with ZenLite2011 and ImageJ and assembled with Adobe Photoshop CS3. Cryosections of adult males were done on a Leica CM 3050 S cryostat and stained with oil red O. Electron microscopy of adult male flies was done on a Philips CM120 equipped with a TemCam 224A slow scan CCD camera. For details, see Supplemental Experimental Procedures.

Selection Scheme for Obesity and Antiobesity Genes

In the primary screen, VDRC GD library transgenic RNAi lines were crossed (in cohorts [co] of 200 lines) against a temperature-sensitive fat storage

tissue-specific driver line (ts-FB-Gal4; Beller et al., 2010) and raised under gene-knockdown-repressed conditions (18°C). Male fly progeny (females for X chromosome RNAi transgene integrations) were kept under gene-knockdown-active conditions (30°C) for 6 days, and subsequently the body fat content (FC) was determined in duplicate groups of five flies each. Primary candidate (c) lines, which gave rise to the most obese and most lean flies within their cohort, (criteria were as follows: $FC_c < \text{average } FC_{co} - 1.5 \times \text{SD } FC_{co}$ for obesity gene candidates, and $FC_c > \text{average } FC_{co} + 1.5 \times \text{SD } FC_{co}$ for antiobesity gene candidates) were retested in additional rounds of screening and scored as class I or II candidates according to the following criteria. Regulator candidates consist of the most lean or most obese flies compared to the average of the primary screen candidates ($Z \text{ score} \leq -1.5$ or ≥ 1.5 ; tested in cohorts of 100 lines; class I). To account for the observed transgene integration effects on body fat content, candidate regulators that cause substantial relative body fat increase or decrease, respectively, compared to control flies carrying the same RNAi effector transgene but no driver transgene, were identified ($Z \text{ score} \leq 2.06$ or ≥ 1.49 for males; $Z \text{ score} \leq 1.45$ or ≥ 1.19 for females; class II). Most class I and II regulators (87%) were validated by retesting their effect on body fat storage in two independent experiments using (i) the primary screen RNAi effector fly line expressed in response to an alternative adult fat body driver (*to-Gal4* for autosomal and *yolk-Gal4* for X chromosome GD lines) and/or (ii) by using a second transgenic RNAi line (VDRG KK or Harvard TRiP collection) targeting the same gene to avoid false positive identifications by RNAi off-target effects. Gene knockdowns, which changed the body fat content by more than 25% compared to controls lacking the driver transgene, received a positive validation score. Candidate genes that (i) reached a validation score of ≥ 2 (out of up to four independent experiments), (ii) were represented by at least one high-quality RNAi transgenic lines ($s19 \text{ score} \geq 0.79$ and CAN repeats < 7), and (iii) were not predicted to function in general RNA interference qualified as confirmed fly obesity or antiobesity genes (Figure 2; Table S1).

Metabolic and Physiological Analyses

Lipid Analysis

Fly body fat content, total body TAG, and DAG were quantified by a coupled colorimetric assay and by thin-layer chromatography, as described in Hildebrandt et al. (2011). For further details, see Supplemental Experimental Procedures.

Carbohydrate Analysis

Circulating hemolymph sugar levels and storage glycogen of adult male flies were quantified based on modified assays described in Sieber and Thummel (2009) and Palanker et al. (2009), respectively. For further details, see Supplemental Experimental Procedures.

Food Intake Analysis

Food intake of ad-libitum-fed and food-restricted adult male flies was determined, as described in Beller et al. (2010). For further details, see Supplemental Experimental Procedures.

Energy Expenditure

The metabolic rate of adult male flies was estimated on the basis of manometric measurement of the CO₂ production, as described in Kucherenko et al. (2011). For further details, see Supplemental Experimental Procedures.

Starvation Assay

Water-only starvation assays were done as described (Grönke et al., 2005), with three cohorts of 15 adult male flies per genotype. For further details, see Supplemental Experimental Procedures.

Locomotor Activity Assay

Spontaneous locomotor activity of adult male flies at 25°C under 12:12LD cycle was determined, as described in Beller et al. (2010). For further details, see Supplemental Experimental Procedures.

Quantitative RT-PCR and Western Blot Analysis

Quantitative RT-PCR analyses, as well as western blot analyses, were done as described (Beller et al., 2010), using anti-STIM (as shown in this work) primary antibodies. For further details, see Supplemental Experimental Procedures.

Statistical Analysis

If not stated otherwise, error bars represent SDs among replicate experiments and the statistical significance of differences between data sets was analyzed using the unpaired t test and expressed as p values.

SUPPLEMENTAL INFORMATION

Supplemental Information includes four figures, three tables, and Supplemental Experimental Procedures and can be found with this article online at <http://dx.doi.org/10.1016/j.cmet.2013.12.004>.

AUTHOR CONTRIBUTIONS

The study was designed by R.P.K. and J.B. The authors J.B., I.B., K.K., M.F., K.M.K., and R.P.K. performed the genetic screen. P.H. contributed the bioinformatics analysis; D.R. performed the electron microscopy, and A.H. performed the TLC analyses. All other experiments were performed by J.B. and analyzed by J.B. and R.P.K. The authors R.P.K., J.B. and H.J. wrote the manuscript.

ACKNOWLEDGMENTS

The authors thank Dr. Aaron Voigt for contributions in the initial phase of this project; Roman Wunderlich, Karin Hartwig and Anja Ebenau for excellent technical assistance; and the Vienna *Drosophila* RNAi Center (VDRG), the Bloomington *Drosophila* Stock Center (BDSC), the TRiP at Harvard Medical School (NIH/NIGMS R01-GM084947), Dr. Justin DiAngelo, Dr. Garry Hime, Dr. Gaiti Hasan, Dr. Laurent Perrin, Dr. Jae Suh, and Dr. Jing Wang for fly stocks. Dr. Pierre Léopold is acknowledged for providing antibodies, Dr. Bernadette Breiden for providing advice on lipid analytics, Dr. April Marrone for providing advice on metabolic-rate analytics, and Hartmut Sebesse for providing artwork. This work was supported by the Max Planck Society.

Received: July 4, 2013

Revised: October 12, 2013

Accepted: November 19, 2013

Published: February 4, 2014

REFERENCES

- Ashrafi, K., Chang, F.Y., Watts, J.L., Fraser, A.G., Kamath, R.S., Ahringer, J., and Ruvkun, G. (2003). Genome-wide RNAi analysis of *Caenorhabditis elegans* fat regulatory genes. *Nature* 421, 268–272.
- Beller, M., Sztalryd, C., Southall, N., Bell, M., Jäckle, H., Auld, D.S., and Oliver, B. (2008). COPI complex is a regulator of lipid homeostasis. *PLoS Biol.* 6, e292.
- Beller, M., Bulankina, A.V., Hsiao, H.-H., Urlaub, H., Jäckle, H., and Kühnlein, R.P. (2010). PERILIPIN-dependent control of lipid droplet structure and fat storage in *Drosophila*. *Cell Metab.* 12, 521–532.
- Britton, J.S., and Edgar, B.A. (1998). Environmental control of the cell cycle in *Drosophila*: nutrition activates mitotic and endoreplicative cells by distinct mechanisms. *Development* 125, 2149–2158.
- Buszczak, M., Lu, X., Segreaves, W.A., Chang, T.Y., and Cooley, L. (2002). Mutations in the midway gene disrupt a *Drosophila* acyl coenzyme A: diacylglycerol acyltransferase. *Genetics* 160, 1511–1518.
- Choquet, H., and Meyre, D. (2011). Molecular basis of obesity: current status and future prospects. *Curr. Genomics* 12, 154–168.
- Colombani, J., Raison, S., Pantalacci, S., Radimerski, T., Montagne, J., and Léopold, P. (2003). A nutrient sensor mechanism controls *Drosophila* growth. *Cell* 114, 739–749.
- Czabany, T., Athenstaedt, K., and Daum, G. (2007). Synthesis, storage and degradation of neutral lipids in yeast. *Biochim. Biophys. Acta* 1771, 299–309.
- Daum, G., Tuller, G., Nemeč, T., Hraštík, C., Balliano, G., Cattel, L., Milla, P., Rocco, F., Conzelmann, A., Vionnet, C., et al. (1999). Systematic analysis of yeast strains with possible defects in lipid metabolism. *Yeast* 15, 601–614.
- Dietzl, G., Chen, D., Schnorrer, F., Su, K.-C., Barinova, Y., Fellner, M., Gasser, B., Kinsey, K., Oettel, S., Scheiblaue, S., et al. (2007). A genome-wide transgenic RNAi library for conditional gene inactivation in *Drosophila*. *Nature* 448, 151–156.

- Fullerton, M.D., Hakimuddin, F., Bonen, A., and Bakovic, M. (2009). The development of a metabolic disease phenotype in CTP:phosphoethanolamine cytidyltransferase-deficient mice. *J. Biol. Chem.* *284*, 25704–25713.
- Géminard, C., Rulifson, E.J., and Léopold, P. (2009). Remote control of insulin secretion by fat cells in *Drosophila*. *Cell Metab.* *10*, 199–207.
- Goodman, J.M. (2009). Demonstrated and inferred metabolism associated with cytosolic lipid droplets. *J. Lipid Res.* *50*, 2148–2156.
- Graham, S.J.L., Black, M.J., Soboloff, J., Gill, D.L., Dziadek, M.A., and Johnstone, L.S. (2009). Stim1, an endoplasmic reticulum Ca²⁺ sensor, negatively regulates 3T3-L1 pre-adipocyte differentiation. *Differentiation* *77*, 239–247.
- Grönke, S., Mildner, A., Fellert, S., Tennagels, N., Petry, S., Müller, G., Jäckle, H., and Kühnlein, R.P. (2005). Brummer lipase is an evolutionary conserved fat storage regulator in *Drosophila*. *Cell Metab.* *1*, 323–330.
- Guo, Y., Walther, T.C., Rao, M., Stuurman, N., Goshima, G., Terayama, K., Wong, J.S., Vale, R.D., Walter, P., and Farese, R.V. (2008). Functional genomic screen reveals genes involved in lipid-droplet formation and utilization. *Nature* *453*, 657–661.
- Haemmerle, G., Lass, A., Zimmermann, R., Gorkiewicz, G., Meyer, C., Rozman, J., Heldmaier, G., Maier, R., Theussl, C., Eder, S., et al. (2006). Defective lipolysis and altered energy metabolism in mice lacking adipose triglyceride lipase. *Science* *312*, 734–737.
- Halaas, J.L., Gajiwala, K.S., Maffei, M., Cohen, S.L., Chait, B.T., Rabinowitz, D., Lallone, R.L., Burley, S.K., and Friedman, J.M. (1995). Weight-reducing effects of the plasma protein encoded by the obese gene. *Science* *269*, 543–546.
- Hildebrandt, A., Bickmeyer, I., and Kühnlein, R.P. (2011). Reliable *Drosophila* body fat quantification by a coupled colorimetric assay. *PLoS ONE* *6*, e23796.
- Hong, S.-H., Lee, K.-S., Kwak, S.-J., Kim, A.-K., Bai, H., Jung, M.-S., Kwon, O.-Y., Song, W.-J., Tatar, M., and Yu, K. (2012). Minibrain/Dyrk1a regulates food intake through the Sir2-FOXO-sNPF/NPY pathway in *Drosophila* and mammals. *PLoS Genet.* *8*, e1002857.
- Jones, B.H., Kim, J.H., Zemel, M.B., Woychik, R.P., Michaud, E.J., Wilkison, W.O., and Moustaid, N. (1996). Upregulation of adipocyte metabolism by agouti protein: possible paracrine actions in yellow mouse obesity. *Am. J. Physiol.* *270*, E192–E196.
- Kahsai, L., Kapan, N., Dirksen, H., Winther, A.M.E., and Nässel, D.R. (2010). Metabolic stress responses in *Drosophila* are modulated by brain neurosecretory cells that produce multiple neuropeptides. *PLoS ONE* *5*, e11480.
- Kohlwein, S.D. (2010). Triacylglycerol homeostasis: insights from yeast. *J. Biol. Chem.* *285*, 15663–15667.
- Kucherenko, M.M., Marrone, A.K., Rishko, V.M., Magliarelli, H. de F., and Shcherbata, H.R. (2011). Stress and muscular dystrophy: a genetic screen for dystroglycan and dystrophin interactors in *Drosophila* identifies cellular stress response components. *Dev. Biol.* *352*, 228–242.
- Lee, K.-S., You, K.-H., Choo, J.-K., Han, Y.-M., and Yu, K. (2004). *Drosophila* short neuropeptide F regulates food intake and body size. *J. Biol. Chem.* *279*, 50781–50789.
- Leonardi, R., Frank, M.W., Jackson, P.D., Rock, C.O., and Jackowski, S. (2009). Elimination of the CDP-ethanolamine pathway disrupts hepatic lipid homeostasis. *J. Biol. Chem.* *284*, 27077–27089.
- Lim, H.-Y., Wang, W., Wessells, R.J., Ocorr, K., and Bodmer, R. (2011). Phospholipid homeostasis regulates lipid metabolism and cardiac function through SREBP signaling in *Drosophila*. *Genes Dev.* *25*, 189–200.
- Mak, H.Y., Nelson, L.S., Basson, M., Johnson, C.D., and Ruvkun, G. (2006). Polygenic control of *Caenorhabditis elegans* fat storage. *Nat. Genet.* *38*, 363–368.
- Masuyama, K., Zhang, Y., Rao, Y., and Wang, J.W. (2012). Mapping neural circuits with activity-dependent nuclear import of a transcription factor. *J. Neurogenet.* *26*, 89–102.
- McAllister, E.J., Dhurandhar, N.V., Keith, S.W., Aronne, L.J., Barger, J., Baskin, M., Benca, R.M., Biggio, J., Boggiano, M.M., Eisenmann, J.C., et al. (2009). Ten putative contributors to the obesity epidemic. *Crit. Rev. Food Sci. Nutr.* *49*, 868–913.
- McGuire, S.E., Le, P.T., Osborn, A.J., Matsumoto, K., and Davis, R.L. (2003). Spatiotemporal rescue of memory dysfunction in *Drosophila*. *Science* *302*, 1765–1768.
- McMenamin, S.K., Minchin, J.E.N., Gordon, T.N., Rawls, J.F., and Parichy, D.M. (2013). Dwarfism and increased adiposity in the gh1 mutant zebrafish vizzini. *Endocrinology* *154*, 1476–1487.
- McNew, J.A., Søgaard, M., Lampen, N.M., Machida, S., Ye, R.R., Lacomis, L., Tempst, P., Rothman, J.E., and Söllner, T.H. (1997). Ykt6p, a prenylated SNARE essential for endoplasmic reticulum-Golgi transport. *J. Biol. Chem.* *272*, 17776–17783.
- Montague, C.T., Farooqi, I.S., Whitehead, J.P., Soos, M.A., Rau, H., Wareham, N.J., Sewter, C.P., Digby, J.E., Mohammed, S.N., Hurst, J.A., et al. (1997). Congenital leptin deficiency is associated with severe early-onset obesity in humans. *Nature* *387*, 903–908.
- Murphy, D.J. (2012). The dynamic roles of intracellular lipid droplets: from archaea to mammals. *Protoplasma* *249*, 541–585.
- Nair, U., Jotwani, A., Geng, J., Gammoh, N., Richerson, D., Yen, W.L., Griffith, J., Nag, S., Wang, K., Moss, T., et al. (2011). SNARE proteins are required for macroautophagy. *Cell* *146*, 290–302.
- Nässel, D.R., and Wegener, C. (2011). A comparative review of short and long neuropeptide F signaling in invertebrates: Any similarities to vertebrate neuropeptide Y signaling? *Peptides* *32*, 1335–1355.
- Natter, K., Leitner, P., Faschinger, A., Wolinski, H., McCraith, S., Fields, S., and Kohlwein, S.D. (2005). The spatial organization of lipid synthesis in the yeast *Saccharomyces cerevisiae* derived from large scale green fluorescent protein tagging and high resolution microscopy. *Mol. Cell. Proteomics* *4*, 662–672.
- Ntambi, J.M., and Takova, T. (1996). Role of Ca²⁺ in the early stages of murine adipocyte differentiation as evidenced by calcium mobilizing agents. *Differentiation* *60*, 151–158.
- Palanker, L., Tennessen, J.M., Lam, G., and Thummel, C.S. (2009). *Drosophila* HNF4 regulates lipid mobilization and β -oxidation. *Cell Metab.* *9*, 228–239.
- Pospisilik, J.A., Schramek, D., Schnidar, H., Cronin, S.J.F., Nehme, N.T., Zhang, X., Knauf, C., Cani, P.D., Aumayr, K., Todoric, J., et al. (2010). *Drosophila* genome-wide obesity screen reveals hedgehog as a determinant of brown versus white adipose cell fate. *Cell* *140*, 148–160.
- Rajan, A., and Perrimon, N. (2012). *Drosophila* cytokine unpaired 2 regulates physiological homeostasis by remotely controlling insulin secretion. *Cell* *151*, 123–137.
- Sandholt, C.H., Hansen, T., and Pedersen, O. (2012). Beyond the fourth wave of genome-wide obesity association studies. *Nutr. Diabetes* *2*, e37.
- Shi, H., Halvorsen, Y.D., Ellis, P.N., Wilkison, W.O., and Zemel, M.B. (2000). Role of intracellular calcium in human adipocyte differentiation. *Physiol. Genomics* *3*, 75–82.
- Sieber, M.H., and Thummel, C.S. (2009). The DHR96 nuclear receptor controls triacylglycerol homeostasis in *Drosophila*. *Cell Metab.* *10*, 481–490.
- Singh, R., Kaushik, S., Wang, Y., Xiang, Y., Novak, I., Komatsu, M., Tanaka, K., Cuervo, A.M., and Czaja, M.J. (2009). Autophagy regulates lipid metabolism. *Nature* *458*, 1131–1135.
- Soboloff, J., Rothberg, B.S., Madesh, M., and Gill, D.L. (2012). STIM proteins: dynamic calcium signal transducers. *Nat. Rev. Mol. Cell Biol.* *13*, 549–565.
- Speliotes, E.K., Willer, C.J., Berndt, S.I., Monda, K.L., Thorleifsson, G., Jackson, A.U., Lango Allen, H., Lindgren, C.M., Luan, J., Mägi, R., et al.; MAGIC; Procardis Consortium (2010). Association analyses of 249,796 individuals reveal 18 new loci associated with body mass index. *Nat. Genet.* *42*, 937–948.
- Subramanian, M., Metya, S.K., Sadaf, S., Kumar, S., Schwudke, D., and Hasan, G. (2013). Altered lipid homeostasis in *Drosophila* InsP3 receptor mutants leads to obesity and hyperphagia. *Dis. Model. Mech.* *6*, 734–744.
- Suh, J.M., Zeve, D., McKay, R., Seo, J., Salo, Z., Li, R., Wang, M., and Graff, J.M. (2007). Adipose is a conserved dosage-sensitive antiobesity gene. *Cell Metab.* *6*, 195–207.

Walther, T.C., and Farese, R.V., Jr. (2012). Lipid droplets and cellular lipid metabolism. *Annu. Rev. Biochem.* *81*, 687–714.

Xue, B., Moustaid, N., Wilkison, W.O., and Zemel, M.B. (1998). The agouti gene product inhibits lipolysis in human adipocytes via a Ca²⁺-dependent mechanism. *FASEB J.* *12*, 1391–1396.

Zechner, R., Zimmermann, R., Eichmann, T.O., Kohlwein, S.D., Haemmerle, G., Lass, A., and Madeo, F. (2012). FAT SIGNALS—lipases and lipolysis in lipid metabolism and signaling. *Cell Metab.* *15*, 279–291.

Zhang, L.L., Yan Liu, D., Ma, L.Q., Luo, Z.D., Cao, T.B., Zhong, J., Yan, Z.C., Wang, L.J., Zhao, Z.G., Zhu, S.J., et al. (2007). Activation of transient receptor potential vanilloid type-1 channel prevents adipogenesis and obesity. *Circ. Res.* *100*, 1063–1070.

Zimmermann, R., Strauss, J.G., Haemmerle, G., Schoiswohl, G., Birner-Gruenberger, R., Riederer, M., Lass, A., Neuberger, G., Eisenhaber, F., Hermetter, A., and Zechner, R. (2004). Fat mobilization in adipose tissue is promoted by adipose triglyceride lipase. *Science* *306*, 1383–1386.